PCCP

UV absorption cross sections of HO_2NO_2 between 343 and 273 K

Gary Knight,† A. R. Ravishankara‡ and James B. Burkholder*

Aeronomy Laboratory, National Oceanic and Atmospheric Administration, 325 Broadway, Boulder, CO 80305–3328, USA. E-mail: Burk@al.noaa.gov

Received 2nd October 2001, Accepted 3rd January 2002
First published as an Advance Article on the web 11th March 2002

The UV absorption spectrum of gas phase HO_2NO_2 (PNA, peroxynitric acid) was measured over the wavelength range 220 to 350 nm at temperatures between 273 and 343 K using a diode array spectrometer. Contributions to the measured spectra from HNO_3, H_2O_2 and NO_2 were subtracted by using mass spectral detection of HNO_3 and H_2O_2 and UV/Vis absorption for NO_2. Our HO_2NO_2 absorption spectra have been scaled to the previously reported absorption cross section data of Molina and Molina [L. T. Molina and M. J. Molina, *J. Photochem.*, 1981, **15**, 97] and Singer *et al.* [R. J. Singer, J. N. Crowley, J. P. Burrows, W. Schneider and G. K. Moortgat, *J. Photochem. Photobiol., A: Chemistry*, 1989, **48**, 17] at 250 nm. Our measured HO_2NO_2 cross sections at wavelengths longer than 290 nm are compared with literature values and the discrepancies are discussed. An empirical parametrization of the measured HO_2NO_2 cross section temperature dependence for use in atmospheric model calculations is presented.

Introduction

Peroxynitric acid (HO_2NO_2, PNA) plays an important role in the colder regions of the troposphere and lower stratosphere as a temporary reservoir for both odd hydrogen, HOx, and nitrogen oxides, NOx (= NO + NO_2). Peroxynitric acid is formed in the atmosphere *via* the reaction

$$HO_2 + NO_2 + M \leftrightarrow HO_2NO_2 + M \qquad (1, -1)$$

The pressure and temperature dependent rate coefficients for the forward and reverse reactions have been measured and evaluated (see DeMore *et al.*[1] and references therein). Processes that remove HO_2NO_2 from the atmosphere include thermal decomposition, k_{-1}, reaction with the OH radical,

$$OH + HO_2NO_2 \rightarrow \text{Products} \qquad (2)$$

and photolysis

$$HO_2NO_2 + h\nu \rightarrow \text{Products} \qquad (3)$$

in the UV[2,3] and near-infrared.[4–6] In the lower troposphere thermal decomposition is often the dominant loss process with a temperature (*i.e.* altitude) dependent lifetime in the range from 20 to 10^5 s. Loss of HO_2NO_2 due to reaction with OH and photolysis become progressively more important with decreasing temperature, *i.e.* in the upper troposphere and lower stratosphere (UT/LS).

Molina and Molina[2] and Singer *et al.*[3] have reported room temperature UV absorption cross sections for HO_2NO_2 between 190 and 330 nm. These studies also contain comprehensive summaries and comparisons with previous HO_2NO_2 cross section studies. An average of the cross sections reported by Singer *et al.* and Molina and Molina is currently recommended for use in atmospheric models.[1] Atmospheric photolysis rates calculated using these cross sections show that UV photolysis is an important loss process for HO_2NO_2 in the UT/LS. The absorption cross section data from these two studies are in very good agreement at wavelengths less than 290 nm. However, in the wavelength region most important for atmospheric photolysis in the UT/LS, *i.e.* > 290 nm, Molina and Molina report cross sections that are significantly larger than those measured by Singer *et al.* These differences in cross sections result in differences in calculated atmospheric UV photolysis rates of nearly a factor of two. In their study, Singer *et al.* also attempted to measure the temperature dependence of the HO_2NO_2 cross section. They observed no measurable change in the cross sections within their measurement precision, at temperatures as low as 253 K and concluded that the cross sections are essentially independent of temperature. The temperature dependence of the absorption cross sections requires further investigation since photolysis of PNA is expected to be most important in the cold regions of the UT/LS.

In this paper, we report UV absorption cross sections for HO_2NO_2 over the wavelength range 220 to 350 nm at temperatures between 273 and 343 K, with an emphasis on wavelengths greater than 290 nm. The higher precision of our measurements enabled us to determine the temperature dependence of the absorption cross sections in this wavelength region. We report a parametrization of the UV absorption cross sections for use in atmospheric model calculations. A few salient points regarding the atmospheric photolysis of HO_2NO_2 in the UV are summarized here while detailed atmospheric loss rate calculations are presented by Stark *et al.*[6]

Experimental section

In this study, we have employed the apparatus and techniques used previously in our laboratory for measuring UV absorption cross sections.[7] The experimental apparatus consisted of four basic components: (1) a UV absorption spectrometer, (2) a small volume absorption cell through which a gas mixture could be flowed rapidly, (3) a reservoir/source of gas phase PNA, and (4) a mass spectrometer for measuring the composition of the gas mixture. A brief description of each of these components is presented separately below.

† Also associated with CIRES, University of Colorado, Boulder, CO 80309, USA.
† Also associated with Department of Chemistry and Biochemistry, University of Colorado, Boulder, CO 80309, USA.

 DOI: 10.1039/b108904h

A 0.5 m spectrometer with a 1024 element diode array detector was used with a 30 W D_2 lamp light source. A 150 grooves mm^{-1} holographic grating (335 nm bandwidth) was used to cover the wavelength range 200 to 535 nm (~1.5 nm resolution). Typical detector exposure times were ~0.2 s and spectra were recorded by co-adding 20 detector readings. The system stability was typically $\sim 2 \times 10^{-4}$ absorbance units over the time required for a spectrum measurement. The diode array system is well suited for spectral measurements of PNA due to its ability to perform rapid high precision measurements over a broad wavelength range. Precise measurements are needed to accurately correct (spectrally subtract) the measured spectra for the unavoidable presence of H_2O_2 and NO_2 impurities in the PNA source (see below).

The detection of scattered light in the spectrometer can influence the determination of weak absorptions. Optical filters positioned between the absorption cell and the spectrometer entrance were used to minimize scattered light. Two filters were used during the course of the measurements: (1) a 280 nm long-pass optical filter and (2) a 25 cm long cell (5 cm diameter) equipped with quartz windows and filled with ~25 Torr of OCS. The OCS filter effectively cut-off wavelengths less than 250 nm from entering the spectrometer. With each filter no scattered light was detected at the long wavelengths.

The absorption cell consisted of a jacketed glass tube (1 cm i.d.) with quartz windows. The windows were flushed with small flows of the carrier gas, constituting ~20% of the total gas flow, to prevent contact and/or condensation of the sample on the windows. The windows were maintained at room temperature during all the measurements. The cell was maintained at a constant temperature by circulating fluid from a temperature-regulated reservoir through the cell jacket. The effective absorption pathlength (gas inlet to outlet) was measured to be 195 cm. The pressure in the absorption cell was 10 Torr. The residence time of the gas sample in the cell was 0.1 s.

Absorption spectra, $A(\lambda) = -\ln(I/I_0)$, were determined by first measuring the lamp spectrum, I_0, while flushing the cell with He. The sample was then introduced into the gas flow and passed through the absorption cell. After the concentration of H_2O_2 in the flow stabilized, after about 30 s, as indicated by the continuously monitored mass spectrometer signal (see below) another spectrum, I, was recorded. The sample flow was then turned off and the absorption cell was flushed with the He flow. Another I_0 spectrum was recorded and compared with the previous baseline spectrum. Only a few measurements which had deviations between the two I_0 measurements greater than the system stability, $A = 0.0002$, were not used in the data analysis.

Mass spectrometer

The mass spectrometer was a commercial residual gas analyzer (RGA). The RGA was equipped with a quadrupole mass filter and an electron impact ionization source. An electron energy of 75 eV was found to have the optimal sensitivity for detection of H_2O_2. The RGA was operated in the selective ion mode to monitor O_2 ($m/z = 32$), H_2O_2 ($m/z = 34$), and HNO_3 ($m/z = 63$).

The RGA sampled the gas flow at the output of the absorption cell through a 40 μm pin-hole. The vacuum connection between the absorption cell and RGA consisted of 1.27 o.d. glass tubing. The gas flow passed directly over the sampling inlet. The pressure in the RGA was $< 5 \times 10^{-5}$ Torr.

The mass spectrometer signals for H_2O_2 and HNO_3 were calibrated relative to the concentrations measured by UV absorption. Calibrations were performed under flow and pressure conditions identical to those used in the PNA experiments. Calibrations were also performed over the same range of H_2O_2 and HNO_3 concentrations observed in the gas flow containing PNA. The mass spectrometer signals varied linearly over this range of concentration. Calibrations for H_2O_2 were performed before and after each PNA spectrum measurement experiment.

Oxygen was observed in the background signal and was also present in the PNA source. Based on the calibrated O_2 signal ($m/z = 32$), a correction of less than 1% was made to the H_2O_2 signal ($m/z = 34$) to account for the presence of ^{18}OO ($m/z = 34$). The O_2 signal was calibrated using measured flow rates and pressures. The detection limit (S/N = 1) for H_2O_2 was $\sim 4 \times 10^{13}$ molecule cm^{-3} for an integration time of 0.5 s. Typically 6 to 10 measurements were averaged during a measurement with a typical standard deviation of ~5% (1σ).

Peroxynitric acid source

Peroxynitric acid was produced by slowly adding 5 g of BF_4NO_2 over a period of 30 min to 10 cm^3 of concentrated (>95%) H_2O_2 held at 273 K.

$$BF_4NO_2 + H_2O_2 \rightarrow BF_3 + HF + HO_2NO_2 \qquad (4)$$

The PNA sample was prepared off-line in a glove-bag purged with dry N_2 and then transferred to a 250 cm^3 glass round bottom flask. Peroxynitric acid was introduced into the UV absorption cell by passing a small flow of He over the surface of the liquid mixture. The PNA source was connected to the absorption cell *via* short sections of Teflon and glass tubing. The PNA source was isolated from the absorption cell with Teflon stopcocks.

The temperature of the PNA source was maintained at 273 K by submersing the reservoir (including the gas headspace) in a water/ice bath. A bath temperature of 273 K was optimum for our measurements because the source did not yield sufficient concentrations of PNA in the gas flow at lower temperatures. Warmer temperatures resulted in higher PNA concentrations but also significantly increased the concentration of NO_2 in the gas flow (see below).

Under our flow and pressure conditions, the reservoir produced high PNA concentrations, $> 1 \times 10^{16}$ molecule cm^{-3}, in the gas flow for only a few minutes. After this initial burst, the PNA concentration in the gas flow decreased into the range $(3\text{–}6) \times 10^{15}$ molecule cm^{-3} from which it slowly decreased over the next hour. Although the initial burst contained the highest PNA concentrations, *i.e.* highest absorption at long wavelengths, the absorption signals due to NO_2 were too high to accurately retrieve the PNA absorption signal at wavelengths >320 nm. Only spectra recorded with PNA concentrations greater than 5×10^{15} molecule cm^{-3} were used to determine the PNA absorption spectrum at wavelengths greater than 330 nm. Still lower PNA concentrations did not provide sufficient absorption at the longer wavelengths to accurately measure its spectrum. After the PNA concentration dropped to $< 3 \times 10^{15}$ molecule cm^{-3} the NO_2 concentration had decreased by as much as a factor of 40 relative to that in the initial burst.

Materials

Helium (UHP, 99.9995%) was used as the carrier gas after it had passed through a molecular sieve trap at liquid nitrogen temperature. Oxygen (UHP, 99.9995%) was used as supplied. Nitric oxide (C.P. grade) was purified by passing it through a silica gel trap at dry ice temperature. The NO_2 sample was prepared and handled as described by Gierczak *et al.*[8] Nitric acid (HNO_3) was prepared by reaction of $NaNO_3$ with concentrated H_2SO_4. The HNO_3 sample was stored under vacuum in a glass bubbler and introduced into the absorption cell by passing a small He flow through the sample. The NO_2BF_4 (95+%) sample was stored at 273 K in an air-tight container and was used as supplied. The H_2O_2 (95%) sample was purified by

vacuum distillation and its purity measured by titration with $KMnO_4$.

Gas flows were measured using calibrated electronic flow meters. Pressure in the absorption cell was measured using a 100 Torr capacitance manometer.

Results and discussion

Reference spectra for HNO_3, H_2O_2, and NO_2 were measured under the identical temperature and pressure conditions used in the measurements of the PNA spectrum. The reference spectra are needed for the analysis of the PNA spectra and also served to validate the measurement procedures.

The measured reference spectra for HNO_3 were in excellent agreement with previous determinations from this laboratory.[7] Absorption cross sections of HNO_3 at wavelengths greater than 290 nm are relatively small and the measured HNO_3 impurity level in the PNA sample was also small, less than 10% of the PNA concentration. Therefore, the contribution of HNO_3 to the measured spectrum of the PNA sample at wavelengths >290 nm was less than 1% (see spectral analysis section).

Lin *et al.*,[9] Molina and Molina,[2] Nicovich and Wine[10] and Vaghjiani and Ravishankara[11] have reported room temperature absorption cross section data for H_2O_2 over the wavelength range 193 to 350 nm. The data from these studies are in reasonable agreement at wavelengths less than 290 nm but show some differences at the longer wavelengths, up to 40% at 330 nm. DeMore *et al.*[1] have recommended using an average of the four data sets for stratospheric modeling. Nicovich and Wine also reported cross sections over the temperature range 285 to 381 K and a parametrization of their data using a two-level model. For the present work, resolution of the discrepancies in the cross sections of H_2O_2 at long wavelength will reduce the uncertainties in the retrieved PNA spectra. Therefore, we have critically evaluated our measured H_2O_2 reference spectra and the literature data.

In Fig. 1 we show our H_2O_2 reference spectra measured at 273, 296, and 343 K. The spectra have been normalized between 250 and 280 nm to the H_2O_2 cross sections reported by Nicovich and Wine (calculated using their parametrization). Our measured spectra at wavelengths greater than 290 nm are in excellent agreement with those reported by Nicovich and Wine for each temperature. The small kink in the calculated spectra near 290 nm is due to a discontinuity in the parametrization given by Nicovich and Wine. Our data agree very well with the room temperature data reported by Molina and Molina.[2] Also shown in Fig. 1 is the room temperature cross sections reported by Vaghjiani and Ravishankara.[11] They reported absolute H_2O_2 cross sections at four atomic lines (213.9, 253.7, 326.1, and 340.4 nm) and a H_2O_2 absorption spectrum recorded using a diode array spectrometer. The single wavelength cross section values are in good agreement with the present work and that of Nicovich and Wine with the exception of the value at 340.4 nm which is a factor of 1.75 larger. Vaghjiani and Ravishankara also reported cross section data (at 5 nm intervals) obtained from a diode array absorption spectrum scaled to the single wavelength measurements. The discrepancies in the 340.4 nm data point are therefore reflected in this data set. The agreement of the present measurements with those of Nicovich and Wine and Molina and Molina implies that the 340.4 nm data point of Vaghjiani and Ravishankara is in error. The present measurements supersede the cross section data reported by Vaghjiani and Ravishankara.

The present measurements have resolved the discrepancies in the long wavelength cross section data for H_2O_2 and we recommend using the parametrization presented by Nicovich and Wine for use in atmospheric model calculations. The good agreement of our data with those of Molina and Molina[2] and Nicovich and Wine[10] for H_2O_2 and Burkholder *et al.*[7] for HNO_3 demonstrates the ability of our apparatus to precisely measure spectral shapes within an estimated uncertainty of $\sim$0.0002 absorbance units.

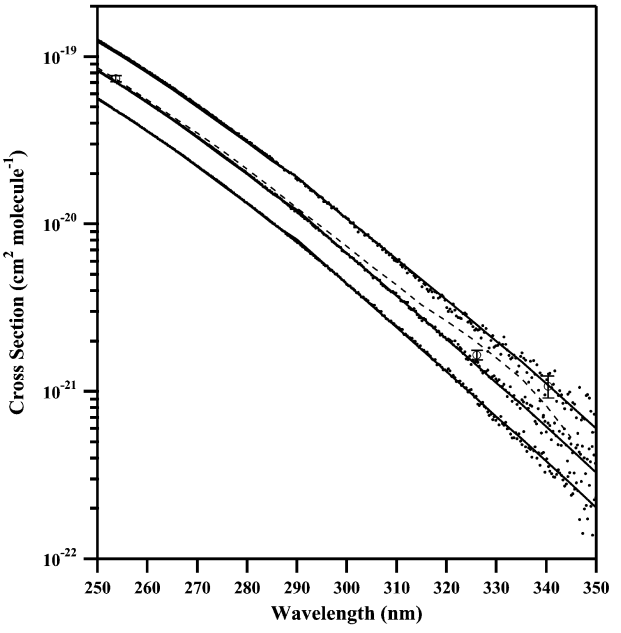

Fig. 1 UV absorption spectra of H_2O_2 measured in this work at 273, 296, and 343 K (dots) compared with the parametrization of the H_2O_2 spectrum reported by Nicovich and Wine[10] (solid lines) and the data from Vaghjiani and Ravishankara[11] (open circles and dashed line). The 273 K spectrum has been shifted down and the 343 K spectrum has been shifted up by 1×10^{-20} cm^2 molecule^{-1} for clarity.

Spectral analysis

Fig. 2 shows a representative PNA spectrum measured at 296 K. Also shown are the contributions of the HNO_3, H_2O_2, and NO_2 impurities that were subtracted from the measured spectrum to obtain the PNA spectrum as the residual. Subtraction of HNO_3 and H_2O_2 were made using measured reference spectra and their concentrations measured using the calibrated mass spectrometer readings. A least-squares fit of the reference NO_2 spectrum between 380 and 480 nm (where it is the only absorbing species in this system) was used to determine the NO_2 concentration. A flat and zero (0.0002 absorbance units) baseline in this wavelength region following the NO_2 subtraction is another test of the stability of the absorption system and validity of our analysis.

The H_2O_2 concentration was measured using the mass spectrometer at the exit of the absorption cell. Therefore, it is important that any gradients in the H_2O_2 concentration along the length of the absorption cell are minimized. The majority of the H_2O_2 observed comes directly from the PNA source itself. However, H_2O_2 can also be formed in the absorption cell *via* the reaction:

$$HO_2 + HO_2 \rightarrow H_2O_2 + O_2 \qquad (5)$$

where HO_2 would be produced by the thermal decomposition of PNA. The H_2O_2 gradient was evaluated by adding NO to the gas flow at the entrance to the absorption cell. The NO scavenged the HO_2 radicals thus preventing the formation of H_2O_2 *via* reaction (5). The H_2O_2 mass spectrometer signal was constant within the precision of the measurements, $\pm$5%, before and after adding NO. However, doubling the residence time in the absorption cell to 0.2 s resulted in a small detectable gradient, $\sim$5%, in the H_2O_2 concentration.

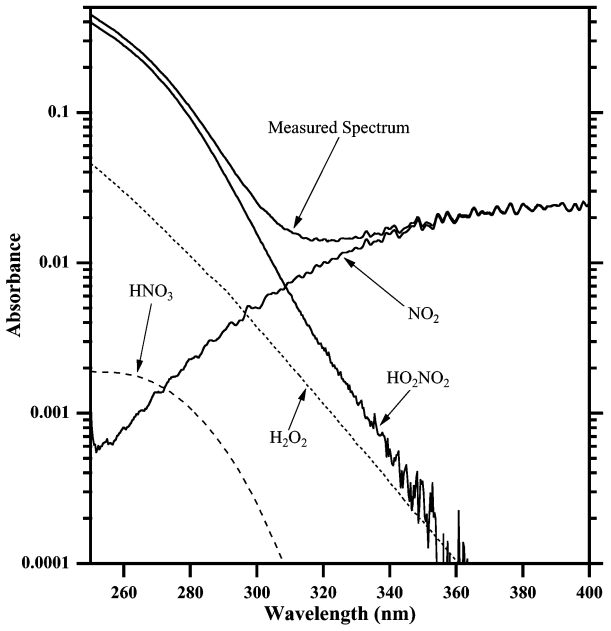

Fig. 2 Typical room temperature UV absorption spectrum measured in this work and results of the spectral analysis for the contributions from HO_2NO_2 (5.16×10^{15} molecule cm^{-3}), H_2O_2 (2.9×10^{15} molecule cm^{-3}), NO_2 (7.3×10^{14} molecule cm^{-3}), and HNO_3 (5×10^{14} molecule cm^{-3}).

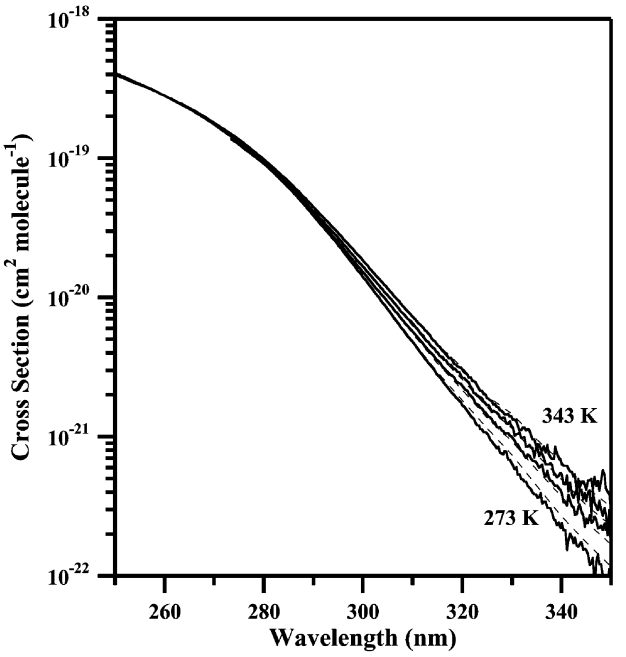

Fig. 3 HO_2NO_2 absorption cross section data at 273, 296, 318, and 343 K. Also shown is the fit to the data (dashed lines) using a two-level model (see text for details).

As is readily seen from Fig. 2, NO_2 and H_2O_2 make large contributions to the total absorption signal (the sum of PNA, H_2O_2, HNO_3, and NO_2) at wavelengths longer than ~310 nm. To better exemplify these contributions, Table 1 lists the relative percent contribution of the PNA sample impurities (H_2O_2, HNO_3, and NO_2) to the total absorption signal at a few wavelengths. The impurity levels varied between measurements but these values are representative of an average measurement. These percent contributions show that accurate and precise spectral subtractions of NO_2 and, to a lesser extent, of H_2O_2 are crucial to an accurate determination of the PNA spectrum. Because of these reasons we employed fast flow conditions during our measurements to minimize the NO_2 concentration in the sample.

Peroxynitric acid absorption spectra were also recorded at three other temperatures (273, 318, and 343 K) using the same methods described above for the 296 K measurements. Spectra were not measured below 273 K because of the low vapor pressure of peroxynitric acid. Rapid thermal decomposition and the consequent production of NO_2 established the high temperature limit, 343 K. The PNA spectra recorded at 273, 296, 318, and 343 K are shown in Fig. 3. Our relative absorbance spectra were placed on an absolute scale using the values of cross sections between 250 and 270 nm reported by Molina and Molina[2] and Singer *et al.*[3] The PNA spectrum shape between 250 and 270 nm was found to be independent of temperature within our measurement precision. Therefore, in our analysis we have assumed that the absorption cross sections in this wavelength range are temperature independent. This analysis shows a systematic decrease in absorption cross section of PNA with decreasing temperature for wavelengths > 280 nm.

Table 1 Fractional contribution by HO_2NO_2, H_2O_2, NO_2, and HNO_3 to the measured absorption spectrum at 296 K for a few select wavelengths.

	Fraction of absorption due to:			
Wavelength/nm	HO_2NO_2	H_2O_2	NO_2	HNO_3
300	0.643	0.148	0.199	0.01
310	0.411	0.128	0.456	0.0048
320	0.211	0.079	0.709	0.0013
330	0.107	0.042	0.851	0.0003
340	0.059	0.020	0.921	0.00007
350	0.0394	0.0106	0.950	0.00002

Atmospheric model calculations of the upper troposphere and lower stratosphere often require absorption cross section data at temperatures as low as 190 K. This presents a problem in the model calculations given that the PNA absorption cross section data have not been measured at these low temperatures. The temperature dependence of the PNA absorption cross sections needs to be included for accurate photolysis rate calculations.[6] Modelers have typically taken the approach of calculating photolysis rates at temperatures below where experimental data are available by using the lowest temperature data available. Sometimes, as in the case of PNA, this approach will introduce systematic errors in the model calculated photolysis rates. Another approach is to use cross section data extrapolated to the lower temperatures. The extrapolation parameters would be based on fits to the measured temperature dependent values. This method can also introduce systematic errors in the calculated photolysis rates depending on the reasonableness of the extrapolation.

We have parameterized the measured temperature dependent cross section data using a simple two component absorption model

$$\sigma(T,\lambda) = \sigma_0(\lambda)/Q + \sigma_1(\lambda)(1 - 1/Q) \qquad (6)$$

where the partition function is given by $Q = 1 + e^{(-\Delta E/(0.69T))}$ where ΔE is in cm^{-1} and T is in K. This parametrization approach has been used previously by Nicovich and Wine[10] in their analysis of the temperature dependence of the UV absorption cross sections of H_2O_2. We have taken $\Delta E = 988$ cm^{-1} (O–O stretch band)[12] in the least squares fitting. The values of $\sigma_0(\lambda)$ and $\sigma_1(\lambda)$ obtained from the fit are given in

Table 2 HO_2NO_2 absorption cross section parametrization

Wavelength/nm	$\sigma(\lambda, 296\ K)/10^{-20}$ [a] cm^2	Wavelength/nm	$\sigma_0(\lambda)/10^{-20}$ cm^2	$\sigma_1(\lambda)/10^{-20}$ cm^2	$\sigma(\lambda, 296\ K)/10^{-20}$ [b] cm^2
190	1010	280	8.73	80.316	9.29
195	816	282	7.5672	76.9384	8.11
200	563	284	6.4044	73.5608	6.93
205	367	286	5.3508	70.6176	5.86
210	241	288	4.4064	68.1088	4.91
215	164	290	3.462	65.6	3.95
220	120	292	2.906	61.5964	3.37
225	95.2	294	2.35	57.5928	2.78
230	80.8	296	1.8924	53.564	2.30
235	69.8	298	1.5332	49.51	1.91
240	59.1	300	1.174	45.456	1.52
245	49.7	302	0.9688	41.13	1.28
250	41.8	304	0.7636	36.804	1.05
255	35.1	306	0.6002	32.7128	0.853
260	27.8	308	0.4786	28.8564	0.702
265	22.4	310	0.357	25	0.551
270	17.8	312	0.2946	22.002	0.465
275	13.4	314	0.2322	19.004	0.380
280	9.30	316	0.1832	16.68	0.313
		318	0.1476	15.03	0.265
		320	0.112	13.38	0.216
		322	0.09576	11.3568	0.184
		324	0.07952	9.33352	0.152
		326	0.0643	8.10646	0.128
		328	0.0501	7.67558	0.110
		330	0.0359	7.2447	0.0926
		332	0.02846	6.43138	0.0788
		334	0.02102	5.61806	0.0650
		336	0.01514	4.95092	0.0540
		338	0.01082	4.42996	0.0456
		340	0.0065	3.909	0.0372
		342	0.00542	3.3866	0.0320
		344	0.00434	2.8642	0.0268
		346	0.0033	2.4781	0.0228
		348	0.0023	2.2283	0.0198
		350	0.0013	1.9785	0.0168

[a] Data taken from Molina and Molina.[2] [b] Calculated using parametrization (see text).

Table 2 and reproduce the experimental data within the measurement uncertainty as shown in Fig. 3.

In this simple picture, using the O–O stretch frequency for the fitting corresponds to photodissociation of HO_2NO_2 into $OH + NO_3$ products. Another reasonable choice for ΔE would be the O_2N–O stretch ($HO_2 + NO_2$ photolysis products), $\Delta E = 514\ cm^{-1}$. However, the overall fits of the temperature dependence using $\Delta E = 514\ cm^{-1}$ were of poorer quality. A measurement of the photolysis quantum yields in the long wavelength region of the PNA spectrum may help in assigning this frequency. At present there are no quantum yield measurements at wavelengths longer than 248 nm available.[13,14] The sensitivity of the photolysis rate calculations to this parametrization is discussed in Stark *et al.*[6]

The absolute accuracy of the PNA absorption cross sections reported in this work were dependent on several factors that include: (1) the accuracy of the absolute cross sections reported by Molina and Molina[2] and Singer *et al.*,[3] (2) the accuracy of our absorption measurements, and (3) the accuracy of the spectral subtraction to take out the contributions of NO_2 and H_2O_2. The accuracy of the absolute cross sections was estimated to be ±10%. Our spectra were normalized to these literature values. If these values are revised in the future our cross section data can be scaled accordingly. We estimate the accuracy of the absorption measurements to be ±0.0002 absorbance units. This will introduce a wavelength dependent uncertainty to the PNA cross section values. The H_2O_2 concentration was measured to within 10% using the calibrated mass spectrometer. The NO_2 spectral subtractions were found to be accurate to within the accuracy of the absorption measurements. Therefore, the major source of uncertainty is the accuracy of the absorption measurements themselves. We estimate the uncertainties of the cross sections given in Table 2 to be 10% for wavelengths less than 300 nm, 15% at 320 nm, and 35% at 340 nm.

Comparison with previous measurements

Molina and Molina[2] and Singer *et al.*[3] have reported PNA absorption cross sections and they appear to be the most accurate to date. These two studies used similar approaches in measuring the PNA spectrum. The absorption cross sections were quantified by chemical titration (Molina and Molina[2]) and mass balance in modulated photolysis experiments (Singer *et al.*[3]). However, the two data sets contain significant discrepancies in the wavelength region of interest in the atmosphere. The source of the differences most likely originates in the accuracy of the spectral corrections for H_2O_2 and NO_2. We have shown in our data analysis that the spectral corrections for H_2O_2 and NO_2 are critical in the determination of the PNA spectrum.

Both Molina and Molina[2] and Singer *et al.*[3] used infrared absorption to quantify HNO_3 and H_2O_2 and UV/visible absorption to quantify NO_2. The UV absorption was measured using scanning monochromators that require several minutes to record an entire absorption spectrum. In their spectral analysis they assumed the sample concentrations were con-

stant for the duration of the measurements. To achieve better sample stability, Singer *et al.* and Molina and Molina both used slow gas flows at atmospheric pressure with residence times in their absorption cells on the order of minutes. The longer residence time allowed the NO_2 concentration to increase through reaction (−1) while the HO_2 radicals were lost *via* the self-reaction (5). Under such conditions, the NO_2 concentration reaches a sufficiently high concentration that reaction (1) essentially stops further loss of PNA. Therefore, a steady-state concentration of PNA is established in the presence of elevated NO_2 concentrations. In contrast, in our approach the cell residence time was short enough to limit the extent of PNA thermal decomposition. The lower NO_2 concentrations achieved in our measurements is the most significant distinction between the present work and previous studies. The NO_2 levels in the experiments of Molina and Molina were about 5 times larger than those encountered in our study, see their Fig. 4. The larger NO_2 levels restricted their measurements to wavelengths below 320 nm. The differences in the NO_2 concentrations in the various studies does not significantly affect the measurements at shorter wavelengths.

The agreement between the Singer *et al.* and Molina and Molina studies is very good at the shorter wavelengths where spectral subtraction due to NO_2 is least important. However, at longer wavelengths the two data sets are in rather poor agreement. Our data in the long wavelength region are in excellent agreement with those of Molina and Molina. We believe our measurements to be the most accurate measurements to date in the atmospherically important wavelength region due to the improved NO_2 spectral subtraction method used (diode array measurements) and the reduced contributions of NO_2 to the absorption signal obtained under fast flow, low pressure conditions.

Conclusions

We have measured UV absorption spectra of PNA between 250 and 350 nm at temperatures in the range 273–343 K. The PNA spectra were placed on an absolute scale by using previously determined absolute cross sections over the wavelength range 250–270 nm. The temperature dependence of the cross section data has been parametrized over this temperature range using a semi-empirical two-level model. A summary of the implications of the revised cross section data on the atmospheric photolysis of PNA is given below. (1) The atmospheric photolysis rate of PNA calculated using room temperature absorption cross section data is ~1.5 times larger than the value obtained using the currently recommended cross section data.[1] (2) Absorption at wavelengths longer than 330 nm, the long wavelength limit reported in previous studies, contribute ~30% to the calculated photolysis rate. (3) The temperature dependence of the PNA cross sections decreases the calculated photolysis rate for a given altitude (over that calculated using room temperature cross section data). Detailed calculations of the photochemical loss of PNA that quantify the above implications are presented in Stark *et al.*[6]

Acknowledgement

This work was funded in part by the upper atmospheric research program of NASA.

References

1 W. B. DeMore, S. P. Sander, D. M. Golden, R. F. Hampson, M. J. Kurylo, C. J. Howard, A. R. Ravishankara, C. E. Kolb and M. J. Molina, *Chemical Kinetics and Photochemical Data for Use in Stratospheric Modeling*, Jet Propulsion Laboratory, Pasadena, CA, USA, 1997, Eval. 12.
2 L. T. Molina and M. J. Molina, *J. Photochem.*, 1981, **15**, 97.
3 R. J. Singer, J. N. Crowley, J. P. Burrows, W. Schneider and G. K. Moortgat, *J. Photochem. Photobiol., A: Chemistry*, 1989, **48**, 17.
4 D. J. Donaldson, G. J. Frost, K. H. Rosenlof, A. F. Tuck and V. Vaida, *Geophys. Res. Lett.*, 1997, **24**, 2651.
5 H. Zhang, C. M. Roehl, S. P. Sander and P. O. Wennberg, *J. Geophys. Res.*, 2000, **105**, 14 593.
6 H. Stark, S. Brown, J. B. Burkholder and A. R. Ravishankara, *Phys. Chem. Chem. Phys.*, 2001, in preparation.
7 J. B. Burkholder, R. K. Talukdar, A. R. Ravishankara and S. Solomon, *J. Geophys. Res.*, 1993, **98**, 22 937.
8 T. Gierczak, J. B. Burkholder and A. R. Ravishankara, *J. Phys. Chem.*, 1999, **103**, 877.
9 C. L. Lin, N. K. Rohatgi and W. B. DeMore, *Geophys. Res. Lett.*, 1978, **5**, 113.
10 J. M. Nicovich and P. H. Wine, *J. Geophys. Res.*, 1988, **93**, 2417.
11 G. L. Vaghjiani and A. R. Ravishankara, *J. Geophys. Res.*, 1989, **94**, 3487.
12 Z. Chen and T. P. Hamilton, *J. Phys. Chem.*, 1996, **100**, 15 731.
13 H. MacLeod, G. P. Smith and D. M. Golden, *J. Geophys. Res.*, 1988, **93**, 3813.
14 C. M. Roehl, T. L. Mazely, R. R. Friedl, Y. Li, J. S. Francisco and S. P. Sander, *J. Phys. Chem. A*, 2001, **105**, 1592.